Evolution of the Uranium Chemical State in Mixed-Valence Oxides

Leinders, G.; Bes, R.; Pakarinen, J.; Kvashnina, K.; Verwerft, M.;

Originally published:

June 2017

Inorganic Chemistry Communications 56(2017)12, 6784-6787

DOI: https://doi.org/10.1021/acs.inorgchem.7b01001

Perma-Link to Publication Repository of HZDR:

https://www.hzdr.de/publications/Publ-25439

Evolution of the Uranium Chemical State in Mixed-Valence Oxides

Gregory Leinders,[1,] René Bes,[2] Janne Pakarinen,[1] Kristina Kvashnina,[3,4] and Marc Verwerft[1]*

[1] Belgian Nuclear Research Centre (SCK•CEN), Institute for Nuclear Materials Science, Boeretang 200, B-2400 Mol, Belgium.

[2] Department of Applied Physics, Aalto University, P.O. Box 14100, FI-00076 Aalto, Finland.

[3] Rossendorf Beamline at ESRF – The European Synchrotron, CS40220, 38043 Grenoble Cedex 9, France

[4] Helmholtz Zentrum Dresden-Rossendorf (HZDR), Institute of Resource Ecology, PO Box 510119, 01314 Dresden, Germany.

AUTHOR INFORMATION

Corresponding Author

*Gregory.leinders@sckcen.be

A fundamental question concerning the chemical state of uranium in the binary oxides UO_2, U_4O_9, U_3O_7, U_3O_8 and UO_3 is addressed. By utilizing high energy resolution fluorescence detection X-ray absorption near edge spectroscopy (HERFD-XANES) at the uranium M_4 edge, a novel technique in the tender X-ray region, we obtain the distribution of formal oxidation states in the mixed valence oxides U_4O_9, U_3O_7 and U_3O_8. Moreover, we clearly identify a pivot from U(IV)-U(V) to U(V)-U(VI) charge compensation, corresponding with transition from a fluorite-type structure (U_3O_7) to a layered structure (U_3O_8). Such physicochemical properties are of interest to a broad audience of researchers and engineers active in domains ranging from fundamental physics, to nuclear industry and environmental science.

TOC GRAPHICS

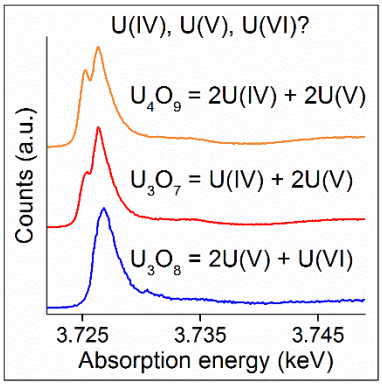

KEYWORDS Uranium oxides, Oxidation state, U_3O_7, HERFD-XANES

Binary uranium oxide compounds, and especially uranium dioxide (UO_2), have been investigated extensively both theoretically and experimentally already for many decades.[1] This world-wide research effort stems not only from their relevance in the frame of safety and economic performance of nuclear power plants,[2, 3] or sustainable nuclear waste management,[4-7] but also originates from a fundamental point of view. The uranium atom contains outer-shell electrons ($5f^3$, $6d^1$, and $7s^2$) located in dispersive and hybridized bands near the Fermi level. Such electronic configuration allows for diverse chemical interactions, including both ionic and covalent bond formation.[8] Furthermore, the near-degeneracy of U 5f, 6d, and 7s orbitals results in a large number of valence electrons available to participate in compound formation.[9]

Uranium oxides show exciting interdependence between their physicochemical properties and complex electronic structures.[10, 11] In particular, the presence of delocalized valence electrons can be seen to stimulate oxidation of UO_2. Accommodation of excess oxygen atoms onto specific sites in the fluorite ($Fm\bar{3}m$) lattice has the potential to increase hybridization between O 2p and U 5f/6d orbitals.[12] The process is dynamic and can result in formation of clusters composed of oxygen atoms and oxygen vacancies.[13, 14] So-called Willis cluster,[15, 16] cuboctahedral oxygen cluster,[17-19] and split-interstitial cluster geometries[12, 20-23] have emerged from the extensive experimental and theoretical work on this topic. However, consensus on the formation and stability of these oxygen clusters has not entirely been reached yet, both between experiment and theoretical calculations,[24, 25] and between different theoretical approaches.[19, 21, 26] It seems that, despite continuing research for more than 70 years, the role of the underlying electronic structure remains difficult to comprehend entirely.

Oxidation of UO_2 modifies the ideal fluorite structure.[6] For oxygen-to-uranium ratios $2 \leq O/U \leq 2.33$, the anion sublattice is strongly affected while the cations keep their fluorite

arrangement.[27] In this range of compositions three main crystallographic phases occur, each exhibiting some degree of non-stoichiometry: UO_{2+x} ($0 \leq x \leq 0.03$), U_4O_{9-y} ($0.02 \leq y \leq 0.06$) and U_3O_{7-z} ($0 \leq z \leq 0.3$).[6, 28, 29] The crystal structures of U_4O_9[1] and U_3O_7 are characterized by long-range ordering of oxygen clusters, which is well established for U_4O_9,[30-32] and recently also a consistent structural model was derived for U_3O_7.[33] At higher O/U values ($2.33 < O/U \leq 3$), the fluorite arrangement of the cations can no longer accommodate the excess anions, and compounds with a layered structure (U_3O_8 and UO_3) are formed.[34, 35]

Charge transfer occurs between valence shells of uranium and the additionally incorporated O^{2-} ions. As a result the uranium-ligand bonding nature modifies, which induces a change in the uranium formal valence state. The occurrence of various oxidation states and different types of chemical bonding has important consequences in the context of nuclear fuel safety and speciation of uranium into the environment. In particular, oxidation of UO_2 is associated with a large volume expansion which can result in rupture of confinement barriers,[6] and additionally, a higher degree of oxidation results in an increased solubility in aqueous environments.[4, 7] Evaluation of the uranium valence mixing in the binary oxides is not straightforward, as charge compensation can be achieved by different oxidation mechanisms, e.g. in U_3O_7:

$U_3O_7 = U(IV) + 2 \times U(V)$ or $2 \times U(IV) + U(VI)$.

In order to better understand the impact of oxidation, accurate evaluation of the uranium oxidation states and their relation to valence electron properties in the oxides is required.

[1]Although exact stoichiometry is excluded in U_4O_{9-y} ($0.02 \leq y \leq 0.06$) the deviation is very small, and hence, in the context of this work the use of the nominal formula U_4O_9 is maintained.

In this study we use high energy resolution fluorescence detection X-ray absorption near edge spectroscopy (HERFD-XANES) at the uranium M_4 edge (i.e. excitation of the $3d_{3/2}$ core electrons) to unambiguously identify formal valence states present in monovalent and mixed-valence uranium compounds by probing the 5f-electron shell configurations. Results on a systematic series of binary uranium oxides are reported, including data measured for the first time on U_3O_7. The stable binary uranium oxides do not present a pure U(V) compound, hence KUO_3 was included in the present assessment as well.

Resonant Inelastic X-ray Scattering (RIXS) maps were recorded for all samples by measuring photon energies around the U Mβ emission line ($3d_{3/2} \rightarrow 4f_{5/2}$, at 3337.4 eV) while scanning the incident energy across the U M_4 edge (~3725 eV). Figure 1 presents a contour plot of the measured intensity in U_3O_7 as a function of incident and transferred photon energies (i.e. the difference between incident and emitted energies). The strong resonance visible near the center of the plot corresponds to the absorption maximum, the so-called white line in the absorption process. The position of the white line on the abscissa distinguishes between the chemical state of uranium ions, whereas the position on the ordinate relates with the binding energy of U $4f_{5/2}$ electrons.

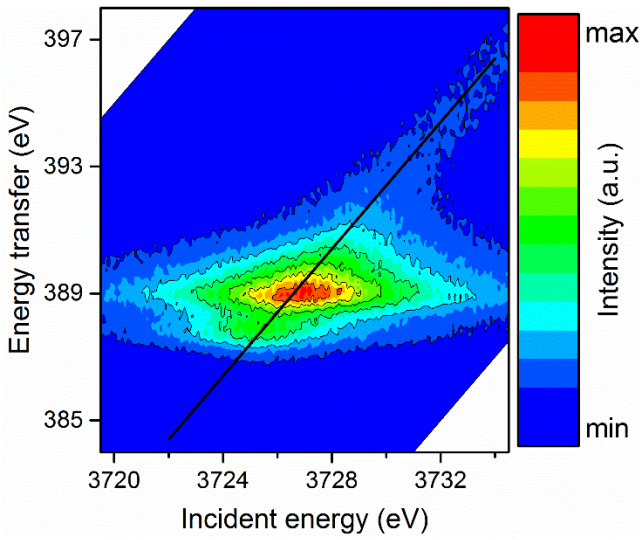

Figure 1. RIXS map of U_3O_7, showing inelastically scattered X-ray intensity as a function of incident and transferred photon energies near the U M_4 absorption edge. A diagonal cut through the maximum corresponds with the HERFD-XANES spectrum measured at the U Mβ fluorescence line.

HERFD-XANES spectra near the U M_4 absorption line correspond to a diagonal cut through the RIXS map, such that the emission energy remains fixed. An overview of the data is shown in Figure 2. The monovalent uranium compounds (UO_2, KUO_3, β-UO_3) clearly display a shift in the position of the absorption maximum. Compared to U(IV), the maximum of the U(V) absorption line is shifted to higher energies by 1.2 eV and for U(VI) by 1.6 eV. The U(VI) absorption spectrum also show a shoulder at the high-energy side about 1 eV from the maximum.

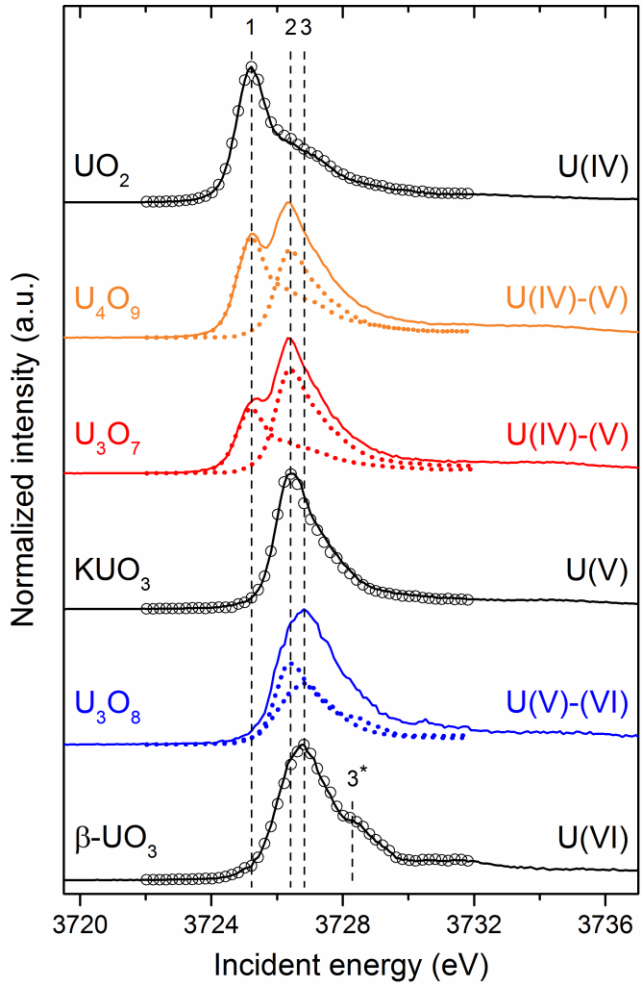

Figure 2. (solid line) HERFD-XANES spectra around the uranium M_4 absorption edge in various uranium oxide compounds. The spectral features denoted by 1-2-3(3^*) relate with the formal valence states U(IV)-U(V)-U(VI), respectively. (dotted lines) Individual component spectra reproduced from the iterative target test, see also **Table 2**, with intensity normalized according to the derived weight fractions.

The UO_2 absorption line has an asymmetrical profile, consisting of a sharp peak around 3725 eV and a shoulder at higher energies. This observation agrees with conventional XANES data reported by other investigators,[36] and it is also reproduced by spectral calculations.[37, 38] The spectrum of KUO_3 also displays slight asymmetry, and shows an increased full-width at half

maximum (FWHM) as compared to that of UO_2, 1.7 eV and 1.4 eV, respectively. It matches closely the HERFD-XANES spectrum of $NaUO_3$ at the U M_4 edge,[39] another monovalent U(V) alkali uranate, a feature which was also observed upon comparing conventional XANES spectra of both compounds at the U L_3 edge.[40] In the spectrum of β-UO_3 additional to line broadening (FWHM = 2.0 eV) a distinctive shoulder appears at about 1 eV from the white line. This shoulder was recognized to be characteristic for uranyl environments (UO_2^{2+}) present in hexavalent uranium systems,[36] and could similarly be reproduced by calculations.[37, 38] As summarized in **Table 1**, the observed spectral features are representative of the chemical shift per oxidation state, i.e. U(IV)-U(V)-U(VI).

Table 1. Overview of incident energy at the position of the white line indicated in Figure 2, corresponding with the formal valence states U(IV)-U(V)-U(VI), and the FWHM measured for all absorption spectra.

	White line energy position (eV), ±0.2 eV			FWHM (eV)
	1	2	3	
UO_2	3725.2	-	-	1.4
U_4O_9	3725.3	3726.4	-	2.7
U_3O_7	3725.4	3726.3	-	2.4
KUO_3	-	3726.4	-	1.7
U_3O_8	-	3726.8		2.2
UO_3	-	-	3726.8*	2.0
Valence	U(IV)	U(V)	U(VI)	

*Additional shoulder visible at 3728.3 eV

The mixed-valence compounds U_4O_9, and U_3O_7 display more complex absorption spectra. In both samples two distinct maxima are distinguished, and the position of both features correspond exactly with the absorption lines of the monovalent compounds UO_2 and KUO_3. Kvashnina *et al*. obtained similar results on a U_4O_9 sample,[37] and attributed the second feature to U(V) because the chemical shift was less than that observed in a hexavalent uranium compound. Here, we find a direct confirmation of this hypothesis via comparison with the KUO_3 spectrum. Interestingly, we measured a ratio of 3:4 in the relative intensity of both spectral features in U_4O_9, which is different from the data reported in Ref. 37 (∼1:1). The discrepancy might be due to the differing sample preparation applied in their research, where some unreacted UO_2 could have remained present.

The HERFD-XANES spectrum of U_3O_7, reported here for the first time, displays the exact same features as observed in U_4O_9, but with a relative intensity ratio of about 1:2. Thus, the U(V) component appears to have increased significantly at the expense of U(IV). One would indeed have expected to see a decrease in the U(IV) component considering the higher degree of oxidation in U_3O_7, but whether this change was balanced via a U(V) or a U(VI) contribution (or both) still remained elusive.[22, 25, 26, 31, 33] The qualitative evaluation of the spectra discussed here shows that U(V) acts as the main charge compensating species both in U_4O_9 and in U_3O_7, and with increasing degree of oxidation the contribution of the U(V) component increases at the expense of U(IV).

The HERFD-XANES spectrum of U_3O_8, another mixed-valence compound, looks different as compared to that of U_4O_9 and U_3O_7. It is more narrow, and the first spectral feature, i.e. the U(IV) component, appears to be absent. Instead, the white line is centered around the U(VI) component, similar as in β-UO_3, but with some asymmetry towards the low-energy side. In the

results of Kvashnina *et al*. this feature appears even more pronounced,[37] and correspondingly, they attributed this to the presence of U(V)-U(VI) oxidation states. From comparison with the chemical shifts observed in the monovalent compounds, and from quantitative analysis reported further, our data similarly suggest presence of U(V)-U(VI) components in the U_3O_8 absorption line. In the past, a distribution of U(IV) and U(VI) in a 1:2 ratio was proposed for U_3O_8, based on the analysis of XPS spectra around the U $N_{6,7}$ edges.[41-43] The current experimental results are in agreement with recent theoretical calculations[22, 25] which indicate that transition from the U(IV)-U(V) to the U(V)-U(VI) regime occurs in-between the U_3O_7 and U_3O_8 compositions, corresponding with the transition from fluorite-type to layered structures.

A quantitative evaluation of the uranium valence state distribution in the mixed-valence compounds (**Table 2**) was performed, utilizing the accurate HERFD-XANES data measured at the U M_4 edge. For this reason the iterative target test (ITT) developed by Rossberg *et al*. and available through their iterative transformation analysis (ITFA) was employed.[44] The method calculates the relative concentrations of components present in each absorption spectrum, given input of at least two known distributions of reference systems such as UO_2 and UO_3. The analysis was restricted to the short HERFD region of the spectra (with incident energy ranging from 3722 to 3732 eV), and constrained the data measured for UO_2, KUO_3, and β-UO_3 to be representative of pure U(IV), U(V), and U(VI) components. Results reported in **Table 2** are completely consistent with the qualitative evaluation of components in the absorption spectra (Figure 2), and are in excellent agreement with values expected from stoichiometric considerations.

Table 2. Distribution of uranium oxidation states in mixed-valence uranium compounds, quantified using ITT on the measured HERFD-XANES U M_4 edge spectra. The average uranium

valence derived from the experimental analysis is in excellent agreement with theoretical values derived from stoichiometric considerations.

	Relative abundance of valence states (%), ± 3%			Average U valence, ±0.03	
	U(IV)	U(V)	U(VI)	Exp.	Theor.
U_4O_9	51	49	0	4.49	4.50
U_3O_7	36	64	0	4.64	4.67
U_3O_8	0	65	35	5.35	5.33

In conclusion, HERFD-XANES at the uranium M_4 edge provides an excellent tool to probe the chemical state of uranium in complex oxides. Our results allow to unambiguously assign U(IV) and U(V) valence states as major components in U_4O_9 and U_3O_7, and also confirm the increasing U(V) contribution at the expense of U(IV) as the degree of oxidation increases ($U_4O_9 \rightarrow U_3O_7$). Significant U(VI) contribution is excluded in these fluorite-type oxides, but a changeover to the U(V)-U(VI) charge compensation mechanism occurs upon further oxidation ($U_3O_7 \rightarrow U_3O_8$). These results finally elucidate the evolution of the uranium chemical state in the binary oxide system, and provide input for further structural and theoretical research on this important class of actinide materials.

EXPERIMENTAL METHODS

The U M_4 edge HERFD−XANES measurements were performed at the ID26 beamline of the European Synchrotron Radiation Facility (ESRF).[45] The U M_4 edge (~3725 eV) incident energy was selected using the Si(111) double-crystal monochromator. Rejection of higher harmonics was achieved by three silicon mirrors at 3.5 mrad working under total reflection. The beam size

was estimated to be ~0.2 mm vertically and 0.5 mm horizontally. HERFD−XANES spectra were measured under cryostat conditions (15 K) using an X-ray emission spectrometer equipped with five Si(220) crystal analyzers and a silicon drift X-ray detector in a vertical Rowland geometry. The spectrometer was tuned to the maximum of the U Mβ ($3d_{3/2} \rightarrow 4f_{5/2}$, at 3337.4 eV) X-ray emission line using the (220) reflection (analyzer crystals at a Bragg angle of ~75.4 °θ). The detected intensity was normalized to the incident flux. The total experimental energy broadening (incident energy convoluted with emitted energy and core-hole lifetime broadening) was evaluated at 0.7 eV.

ASSOCIATED CONTENT

Supporting Information. The Supporting Information is available free of charge via the Internet at http://pubs.acs.org.

Details on sample preparation. (PDF)

AUTHOR INFORMATION

Notes

The authors declare no competing financial interests.

ACKNOWLEDGMENT

The authors wish to thank Sara Lafuerza for her helpful support during the synchrotron experiments at the ID26 beamline (ESRF).

REFERENCES

(1) I. Grenthe, J. Drozdzynski, T. Fujino, E. C. Buck, T. E. Albrecht-Schmitt, S. F. Wolf, *The chemistry of the Actinide and Transactinide elements, Vol. 1*, 3 ed., Springer, Dordrecht, **2006**.

(2) T. Abe, K. Asakura, *2.15 - Uranium Oxide and MOX Production* in *Comprehensive Nuclear Materials*, Elsevier, Oxford, **2012**, pp. 393.
(3) IAEA, *Status and trends of nuclear technologies*, Report IAEA, Vienna, **2009**.
(4) D. J. Wronkiewicz, J. K. Bates, S. F. Wolf, E. C. Buck, Ten-year results from unsaturated drip tests with UO2 at 90°C: implications for the corrosion of spent nuclear fuel. *J. Nucl. Mater.* **1996**, *238*, 78.
(5) G. Bernhard, G. Geipel, V. Brendler, H. Nitsche, Uranium speciation in waters of different uranium mining areas. *J. Alloys Compd.* **1998**, *271–273*, 201.
(6) R. J. McEachern, P. Taylor, A review of the oxidation of uranium dioxide at temperatures below 400 °C. *J. Nucl. Mater.* **1998**, *254*, 87.
(7) D. W. Shoesmith, Fuel corrosion processes under waste disposal conditions. *J. Nucl. Mater.* **2000**, *282*, 1.
(8) H. Y. Geng, Y. Chen, Y. Kaneta, M. Iwasawa, T. Ohnuma, M. Kinoshita, Point defects and clustering in uranium dioxide by LSDA+U calculations. *Phys. Rev. B* **2008**, *77*, 104120.
(9) S. Cotton, *Lanthanide and Actinide Chemistry*, Wiley, Chichester, **2006**.
(10) J. E. Stubbs, A. M. Chaka, E. S. Ilton, C. A. Biwer, M. H. Engelhard, J. R. Bargar, P. J. Eng, UO2 oxidative corrosion by nonclassical diffusion. *Phys. Rev. Lett.* **2015**, *114*, 246103.
(11) S. D. Conradson, D. A. Andersson, P. S. Bagus, K. S. Boland, J. A. Bradley, D. D. Byler, D. L. Clark, D. R. Conradson, F. J. Espinosa-Faller, J. S. Lezama Pacheco, M. B. Martucci, D. Nordlund, G. T. Seidler, J. A. Valdez, Anomalous dispersion and band gap reduction in UO2+x and its possible coupling to the coherent polaronic quantum state. *Nucl. Instrum. Methods Phys. Res., Sect. B* **2016**, *374*, 45.
(12) D. A. Andersson, J. Lezama, B. P. Uberuaga, C. Deo, S. D. Conradson, Cooperativity among defect sites in AO2+x and A4O9 (A=U, Np, Pu): Density functional calculations. *Phys. Rev. B* **2009**, *79*, 024110.
(13) B. T. M. Willis, Structures of UO_2, UO_{2+x} and U_4O_9 by neutron diffraction. *J. Phys. (Paris)* **1964**, *25*, 431.
(14) B. T. M. Willis, Crystallographic studies of anion-excess uranium oxides. *J. Chem. Soc., Faraday Trans. II* **1987**, *83*, 1073.
(15) B. T. M. Willis, The defect structure of hyper-stoichiometric uranium dioxide. *Acta Crystallogr. A* **1978**, *34*, 88.
(16) G. C. Allen, P. A. Tempest, Linear ordering of oxygen clusters in hyperstoichiometric uranium dioxide. *J. Chem. Soc., Dalton Trans.* **1982**, 2169.
(17) D. J. M. Bevan, I. E. Grey, B. T. M. Willis, The crystal structure of β-U_4O_{9-y}. *J. Solid State Chem.* **1986**, *61*, 1.
(18) H. Y. Geng, Y. Chen, Y. Kaneta, M. Kinoshita, Stability mechanism of cuboctahedral clusters in UO2+x: First-principles calculations. *Phys. Rev. B* **2008**, *77*, 180101.
(19) E. Yakub, C. Ronchi, D. Staicu, Computer simulation of defects formation and equilibrium in non-stoichiometric uranium dioxide. *J. Nucl. Mater.* **2009**, *389*, 119.
(20) H. Y. Geng, Y. Chen, Y. Kaneta, M. Kinoshita, Ab initio investigation on oxygen defect clusters in UO2+x. *Appl. Phys. Lett.* **2008**, *93*, 201903.
(21) D. A. Andersson, F. J. Espinosa-Faller, B. P. Uberuaga, S. D. Conradson, Stability and migration of large oxygen clusters in UO2+x: Density functional theory calculations. *J. Chem. Phys.* **2012**, *136*, 234702.

(22) N. A. Brincat, M. Molinari, G. C. Allen, M. T. Storr, S. C. Parker, Density functional theory calculations of defective UO_2 at U_3O_7 stoichiometry. *J. Nucl. Mater.* **2015**, *467*, 724.
(23) K. Govers, S. Lemehov, M. Hou, M. Verwerft, Comparison of interatomic potentials for UO2. Part I: Static calculations. *J. Nucl. Mater.* **2007**, *366*, 161.
(24) A. D. Murray, B. T. M. Willis, A neutron diffraction study of anion clusters in nonstoichiometric uranium dioxide. *J. Solid State Chem.* **1990**, *84*, 52.
(25) D. A. Andersson, G. Baldinozzi, L. Desgranges, D. R. Conradson, S. D. Conradson, Density functional theory calculations of UO_2 oxidation: Evolution of UO_{2+x}, U_4O_{9-y}, U_3O_7, and U_3O_8. *Inorg. Chem.* **2013**, *52*, 2769.
(26) N. A. Brincat, M. Molinari, S. C. Parker, G. C. Allen, M. T. Storr, Computer simulation of defect clusters in UO2 and their dependence on composition. *J. Nucl. Mater.* **2015**, *456*, 329.
(27) B. T. M. Willis, Point defects in uranium oxides. *Proc. Brit. Ceram. Soc.* **1964**, *No. 1*, 9.
(28) C. Rocanière, J. P. Laval, P. Dehaudt, B. Gaudreau, A. Chotard, E. Suard, Structural study of $(U_{0.90}Ce_{0.10})_4O_{9-\delta}$, an anion-excess fluorite superstructure of $U_4O_{9-\delta}$ type. *J. Solid State Chem.* **2004**, *177*, 1758.
(29) G. Leinders, J. Pakarinen, R. Delville, T. Cardinaels, K. Binnemans, M. Verwerft, Low-temperature oxidation of fine UO_2 powders: A process of nanosized domain development. *Inorg. Chem.* **2016**, *55*, 3915.
(30) R. I. Cooper, B. T. M. Willis, Refinement of the structure of β-U_4O_9. *Acta Crystallogr. A* **2004**, *60*, 322.
(31) L. Desgranges, G. Baldinozzi, G. Rousseau, J.-C. Nièpce, G. Calvarin, Neutron diffraction study of the in situ oxidation of UO_2. *Inorg. Chem.* **2009**, *48*, 7585.
(32) L. Desgranges, G. Baldinozzi, D. Simeone, H. E. Fischer, Refinement of the alfa-U4O9 Crystalline Structure: New Insight into the U4O9 -> U3O8 Transformation. *Inorg. Chem.* **2011**, *50*, 6146.
(33) G. Leinders, R. Delville, J. Pakarinen, T. Cardinaels, K. Binnemans, M. Verwerft, Assessment of the U3O7 Crystal Structure by X-ray and Electron Diffraction. *Inorg. Chem.* **2016**, *55*, 9923.
(34) H. R. Hoekstra, S. Siegel, The uranium-oxygen system: U3O8-UO3. *J. Inorg. Nucl. Chem.* **1961**, *18*, 154.
(35) B. Loopstra, The structure of β-U_3O_8. *Acta Crystallogr. B* **1970**, *26*, 656.
(36) J. Petiau, G. Calas, D. Petitmaire, A. Bianconi, M. Benfatto, A. Marcelli, Delocalized versus localized unoccupied 5f states and the uranium site structure in uranium oxides and glasses probed by x-ray-absorption near-edge structure. *Phys. Rev. B* **1986**, *34*, 7350.
(37) K. O. Kvashnina, S. M. Butorin, P. Martin, P. Glatzel, Chemical state of complex uranium oxides. *Phys. Rev. Lett.* **2013**, *111*, 253002.
(38) K. O. Kvashnina, F. M. F. de Groot, Invisible structures in the X-ray absorption spectra of actinides. *J. Electron Spectrosc. Relat. Phenom.* **2014**, *194*, 88.
(39) S. M. Butorin, K. O. Kvashnina, A. L. Smith, K. Popa, P. M. Martin, Crystal-Field and Covalency Effects in Uranates: An X-ray Spectroscopic Study. *Chemistry – A European Journal* **2016**, *22*, 9693.
(40) A. V. Soldatov, D. Lamoen, M. J. Konstantinović, S. Van den Berghe, A. C. Scheinost, M. Verwerft, Local structure and oxidation state of uranium in some ternary oxides: X-ray absorption analysis. *J. Solid State Chem.* **2007**, *180*, 54.

(41) S. D. Senanayake, R. Rousseau, D. Colegrave, H. Idriss, The reaction of water on polycrystalline UO2: Pathways to surface and bulk oxidation. *J. Nucl. Mater.* **2005**, *342*, 179.
(42) J. J. Pireaux, J. Riga, E. Thibaut, C. Tenret-Noel, R. Caudano, J. J. Verbist, Shake-up satellites in the x-ray photoelectron spectra of uranium oxides and fluorides. A band structure scheme for uranium dioxide, UO2. *Chem. Phys.* **1977**, *22*, 113.
(43) J. Verbist, J. Riga, J. J. Pireaux, R. Caudano, X-ray photoelectron spectra of uranium and uranium oxides. Correlation with the half-life of 235Um. *J. Electron. Spectrosc. Relat. Phenom.* **1974**, *5*, 193.
(44) A. Rossberg, K.-U. Ulrich, S. Weiss, S. Tsushima, T. Hiemstra, A. C. Scheinost, Identification of Uranyl Surface Complexes on Ferrihydrite: Advanced EXAFS Data Analysis and CD-MUSIC Modeling. *Environ. Sci. Technol.* **2009**, *43*, 1400.
(45) C. Gauthier, V. A. Sole, R. Signorato, J. Goulon, E. Moguiline, The ESRF beamline ID26: X-ray absorption on ultra dilute sample. *J. Synchrotron Rad.* **1999**, *6*, 164.